

The dynamics of superfluid ^4He

W. Montfrooij

*Department of Physics and the Missouri Research Reactor,
University of Missouri, Columbia Missouri, USA*

E.C. Svensson

*National Research Council Canada,
Chalk River Laboratories, Chalk River Ontario, Canada*

R. Verberg

Chemical Engineering Department, University of Pittsburgh, Pittsburgh Pennsylvania, USA

R.M. Crevecoeur and I.M. de Schepper

Interfaculty Reactor Institute, Mekelweg 15, 2629 JB Delft, The Netherlands

(Dated: February 4, 2008)

Abstract

We present neutron scattering results for the dynamic response by superfluid and normal-fluid ^4He and the results of a simple perturbation-theory analysis which allows us to describe all aspects of the observed behavior by considering only density fluctuations. We show that the three key features that are characteristic of the dynamic response of superfluid ^4He , as well as their dramatic variations with temperature, can be attributed predominantly to the Bose statistics obeyed by all the ^4He atoms. It appears that the presence of the Bose condensate exerts at most a minor influence on the dynamic response.

PACS numbers: 67.40.-w, 05.30.Jp

More than 6 decades after the discovery^{1,2} of superfluidity in liquid ^4He at temperatures below $T_\lambda = 2.17$ K, and the almost immediate intriguing proposal³ that its origin lay in the then obscure phenomenon of Bose-Einstein condensation⁴, we still do not have an all-encompassing theory of superfluid ^4He . The existence of a Bose condensate in superfluid ^4He has since been confirmed^{5,6}, and the current⁷ estimate is that about 10% of the ^4He atoms are condensed into the zero-momentum state at $T \leq 1$ K. In a recent attempt^{8,9,10} to develop a microscopic theory for liquid ^4He , the Bose condensate has been deemed to be of central importance in determining the dynamic response in the superfluid phase. However, key predictions of this theory are inconsistent^{11,12} with observed behavior.

On the other hand, the correlated basis function (CBF) approach to the superfluid state, which has its origin in the works of Feynman¹³ and Jackson and Feenberg^{14,15} and which has since been developed by various groups^{16,17,18,19,20,21}, shows that the elementary excitations of superfluid ^4He can be calculated using a perturbative expansion based on excited states generated by the density operator. Good agreement between calculated and observed excitation energies has now been established^{19,20}. In this paper, we use the CBF-theory results to forward a unified description of all three components in the dynamic response (elementary excitations, multiphonon and recoil scattering) and the variations with temperature thereof. Ever since the Landau's²² prediction of the famous phonon-roton dispersion relation for the elementary excitations, a large body of inelastic neutron scattering work has been accumulated (see^{9,10} for references), revealing the unique features of superfluid ^4He in ever increasing detail. Using the MARI spectrometer at the ISIS pulsed neutron facility, we have extended recent measurements^{23,24,25} to cover a larger dynamic and temperature range, focussing on the region where the excitation curve splits up into three branches. Results for the dynamic response functions at saturated vapor pressure (SVP) are shown in Fig. 1.

At the lowest temperature ($T = 1.35$ K, top panels of Fig. 1), the spectra show three distinct features characteristic of the superfluid phase. First, one observes the phonon-roton dispersion curve with the very intense roton excitations seen as the bright yellow region in Fig. 1. We show (a compilation^{25,26,27} of) the energies and spectral weights of these excitations in Fig. 2. Their lifetimes (related to the reciprocal of their intrinsic energy widths in the neutron spectra) are determined by the number of thermally excited quasiparticles²⁸ present at that temperature, which in turn govern the frequency of collisions between the quasiparticles. At $T = 1.35$ K, the observed widths primarily reflect the instrumental reso-

lution function (FWHM < 0.25 meV). Note also that there is no scattering at energies below the phonon-roton dispersion curve.

Second, as a reddish band above and beyond the roton region in Fig. 1 (and stars in Fig. 2), one observes a broad (in energy) response centred near the recoil energy $\hbar\epsilon_r = \hbar^2 q^2 / 2m$, clearly separated from the scattering on the phonon-roton dispersion curve. This component of the response, from which the Bose condensate fraction can be extracted^{5,7}, mainly reflects the behavior of the individual ^4He atoms.

Third, there is the possibility of a neutron simultaneously exciting multiple quasiparticles. This multiphonon can be observed as a band of (weak) intensity located just above the phonon-roton dispersion curve and merging into the recoil scattering at larger q .

In contrast, the normal-fluid dynamic response (bottom panels of Fig. 1) does not show any sharp excitations, nor is there any separation between the high energy recoil scattering and the low energy response. In addition, line-shape analysis of these and earlier¹² results indicates that the multiphonon component is absent, or at least vanishingly small in the normal-fluid phase. We first discuss how the features of the spectra at the lowest temperature can be understood using (only) perturbation theory and Bose statistics.

The shape of the phonon-roton dispersion curve is sufficient to ensure that the fluid is a superfluid. Specifically, the finite energy gap (roton-minimum at $q_r = 1.92 \text{ \AA}^{-1}$; gap $\Delta = 0.74 \text{ meV} = 8.6 \text{ K}$) means that a minimum velocity (given by the slope of the dashed line in the top panel of Fig. 2) is required in order to excite a roton out of the ground state, with frictionless superflow for lower velocities. As Feynman pointed out¹³, the presence of the energy gap is a direct consequence of the symmetry requirements placed on the wavefunction by the Bose statistics obeyed by the ^4He atoms. This energy gap also ensures that there can be only a few thermally excited quasiparticles at the lowest temperatures, which in turn leads to the long lifetime of the quasiparticles because of the vastly reduced collision frequency between them²⁸. This explains the sharpness of the phonon-roton excitations, and, by consequence, also the full set of features observed in the dynamic response function, as we shall now demonstrate.

Using perturbation theory, it is straightforward to derive a shape for the spectral response consistent with the observed spectra. Following Feynman¹³, we start with a variational estimate for the excited state $|q\rangle$ by letting the density operator ρ_q , which creates a density fluctuation of wavelength $2\pi/q$ somewhere in the liquid, act on the ground state: $|q\rangle = \rho_q^+ |0\rangle$.

The energy of this state is $\hbar\epsilon_F(q) = (q|H|q)/(q|q) = \hbar^2q^2/2mS_q$, with S_q being the static structure factor.

We correct this state by including the two-quasiparticle states $|lm\rangle = \rho_l^+\rho_m^+|0\rangle$. In the following, we use the symbols $|q\rangle$ and $|lm\rangle$ to indicate that the states have been orthonormalized. The corrected excited state energies are now given by the poles of the corresponding Green function G_1 , defined by

$$G_1 = [\omega - \epsilon_F(q) - \Sigma(q, \omega)]^{-1}. \quad (1)$$

Given suitable expressions for the interaction matrix elements $\langle q|H|lm\rangle$ present in the self-energy Σ , the above equation can be solved in an iterative manner, and good agreement with the observed phonon-roton dispersion curve has been obtained for $q < 3\text{\AA}^{-1}$.^{19,20}

The validity of the above set of equations is readily demonstrated by performing a self-consistency check. We calculate the $\langle q|H|lm\rangle$ using a combination^{14,20} of convolution (for $q < 2\text{\AA}^{-1}$) and superposition approximations ($q > 2\text{\AA}^{-1}$). The self-energy is calculated at $T = 0$ K using the observed excitation energies ϵ_{obs} as input, yielding the corrected excitation energies $\epsilon_F(q) - \Sigma(q, \omega = \epsilon_{obs}(q))$ [which ideally would coincide with $\epsilon_{obs}(q)$]. We plot these corrected energies, together with their corresponding intensities, as solid lines in Fig. 2. Clearly, the agreement with experiment is good, even near the end of the dispersion where the corrections to $\epsilon_F(q)$ are very large. The discrepancies reflect inaccuracies in the approximations for the matrix elements, and the neglecting of states with more than two excitations.

Since our primary aim in this paper is to elucidate the basic mechanisms governing the dynamic response of ^4He instead of discussing the details of the interaction, we limit our discussion in the following to a simplified model, which nevertheless still contains the essential physics. Since the model reproduces the correct general *shape* of Σ , it will prove to be sufficient for interpreting the experimental results. In this model, we only consider two-quasiparticle states with momenta l and m near the roton minimum and we replace the matrix elements in this region by an effective $M_{eff}(q)$. As before, we replace the energy dependent corrected energies entering the self-energy Σ by the observed excitation energies $\hbar\epsilon_{obs}$ and lifetimes $\hbar\Gamma$, yielding

$$\Sigma(q, \omega) = \frac{1}{2} \sum_{l,m} \frac{|M_{eff}(q)|^2 \delta_{\vec{q}, \vec{l} + \vec{m}}}{\omega - \epsilon_{obs}(l) - \epsilon_{obs}(m) - 2i\Gamma}. \quad (2)$$

Determining the poles of G_1 can now be done by finding the roots of the much simplified complex equation $\omega + i\eta = \epsilon_F(q) + \Sigma(q, \omega + i\eta)$.

We show the solution in Fig. 3 for $q= 2.3$ and 2.7\AA^{-1} ($M_{eff}(q)$ was fixed by imposing self-consistency on the corrected excitation energies). One observes that the equation yields two solutions due to the appearance of a strong resonance in the selfenergy at 2Δ , i.e., at twice the roton energy. This pronounced resonance is a *direct* consequence of the high density of states near the roton minimum in combination with the long lifetimes of the elementary excitations. For q -values beyond the roton ($q \gtrsim 2.5\text{\AA}^{-1}$). Eq. 1 yields one solution with excitation energy near $\hbar\epsilon_F(q)$ ($\simeq \hbar\epsilon_r$ in this region) and one solution which asymptotically approaches 2Δ , almost independent of the actual values of $\epsilon_F(q)$ and $M_{eff}(q)$. This is exactly what is observed^{25,27} in experiment (see Fig. 2). Note that the linewidth of the solution near 2Δ is roughly given by twice the roton linewidth, as follows directly from Eq. 2 since the imaginary part of the denominator is given by twice the roton linewidth. This linewidth is still very small at $T < 1$ K.

For lower q -values a similar process takes place, resulting in the lowering of the excitation energies with respect to $\epsilon_F(q)$ (see Fig. 2) and in the hybridization of the excitations making up the recoil component and the phonon-roton excitations near $q= 2.3 \text{\AA}^{-1}$. Of course, the two-roton resonance disappears once q approaches $2q_r$ (see Eq. 2). To illustrate how realistic this simplified model still is, we show the predicted intensities Z_q as a dashed curve in the lower part of in Fig. 2. The model thus shows, for all the excitations that constitute the phonon-roton dispersion curve, that the excitations are density fluctuations in character. They are *not* the result of knocking an atom out of the Bose condensate^{8,9,10}. The corrected excited state vectors are also determined in the standard manner²¹. We illustrate in Fig. 4 how this gives rise to the appearance of a multiphonon component. The corrected single quasiparticle excited states $|\psi_q\rangle$ are obtained by rotating $|q\rangle$ in the Hilbert space spanned by $[|q\rangle, \{|lm\rangle\}]$. Whereas the uncorrected states $|lm\rangle$ were orthogonal to $|q\rangle$, the corrected states $|\lambda\mu\rangle$ are orthogonal to $|\psi_q\rangle$ (thus, $\langle \lambda\mu|q\rangle \neq 0$). Since the neutron scattering cross-section of a state $|\cdot\rangle$ is proportional to $|\langle \cdot|q\rangle|^2$, the multi-quasiparticle states can so be directly populated by neutrons, leading to the observed multiphonon component.

We now briefly summarize the observed changes in the neutron spectra on increasing the temperature. There is an increasingly rapid decrease in the lifetime of the excitations¹² as

one approaches T_λ (see Fig. 1). This can be attributed solely to an increase in the collision frequency resulting from the greater number of thermally excited quasiparticles²⁸, there is no need to invoke depletion of the Bose condensate. The intensity in the multiphonon component is transferred to the broadened single excitation¹². The separation between the phonon-roton dispersion curve and the recoil component first weakens and then disappears (see Fig. 1). The excitations near the two-roton threshold rapidly broaden (with at least twice the roton linewidth²⁵) and weaken in intensity.

We can understand the above changes, at least qualitatively, from the results of the simple model. When the lifetime of the roton decreases, the two-roton resonance will become less pronounced. As discussed above, it follows directly from our model that the linewidths of the excitations near the end of the phonon-roton dispersion curve ($q \gtrsim 2.5 \text{ \AA}^{-1}$) increase twice as fast as the roton linewidth increases. In addition, by repeating the model calculations using increased roton linewidths, it follows that their intensities diminish with increasing linewidth so that these excitations can no longer be separated from the recoil component²⁵ (see Fig. 1). Also, with the weakening of the two-roton resonance, the excited state energies will be closer to $\hbar\epsilon_F(q)$. As a consequence, the excited states $|\psi_q\rangle$ will more closely resemble a simple density fluctuation $|q\rangle$, meaning that the multiphonon states $|\lambda\mu\rangle$ will have a smaller weight (or even no weight at all) in the neutron scattering spectra (see Fig. 4). The weakening of the two-roton resonance is probably also the reason why the hybridization weakens (since it is the origin of the hybridization in the first place), but the simple model we have used here is not sufficiently accurate to allow one to follow these effects into the region close to the superfluid transition where the damping rates become comparable to the excitation energies¹².

In summary, the results of our inelastic neutron scattering experiments and our calculations using perturbation theory are in good qualitative agreement. All three key features of the observed spectra in the superfluid phase are fully explained by the long lifetimes of the elementary excitations, and the changes on increasing the temperature can be attributed to the weakening of the two-roton resonance, the latter having its origin in the decreasing lifetime of the roton excitations. Our conclusion is that the dynamic response of superfluid ^4He is determined (primarily) by density fluctuations and that, although a Bose condensate exists in superfluid ^4He , it plays at most a minor role in determining this response.

Acknowledgments

We thank the technical staff at ISIS for their expert assistance during the experiments. This research was supported by the Netherlands Organization for Scientific Research (NWO).

-
- ¹ P. Kapitza, *Nature* **141**, 74 (1938).
 - ² J.F. Allen, and A.D. Misener, *Nature* **141**, 75 (1938).
 - ³ F. London, *Nature* **141**, 643 (1938).
 - ⁴ A. Einstein, *Sitzungsber Berlin Preuss. Akad. Wiss.* 3 (1925).
 - ⁵ V.F. Sears, E.C. Svensson, P. Martel, and A.D.B. Woods, *Phys. Rev. Lett.* **49** 279 (1982).
 - ⁶ A.F.G Wyatt, *Nature* **391**, 56 (1998).
 - ⁷ P.E. Sokol in *Bose-Einstein Condensation* (eds. Griffin, A., Snoke, D.W. & Stringari, S.) p. 51 (Cambridge Univ. Press, 1995).
 - ⁸ H.R. Glyde, and A. Griffin, *Phys. Rev. Lett.* **65** 1454 (1990).
 - ⁹ A. Griffin, *Excitations in a Bose-Condensed Liquid* (Cambridge Univ. Press, 1993).
 - ¹⁰ H.R. Glyde, *Excitations in Liquid and Solid Helium* (Oxford Univ. Press, 1994).
 - ¹¹ E.C. Svensson, W. Montfrooij, and I.M. de Schepper, *Phys. Rev. Lett.* **77**, 4398 (1995); **80**, 2017 (1998).
 - ¹² W. Montfrooij, E.C. Svensson, I.M. de Schepper, and E.G.D. Cohen, *J. Low Temp. Phys.* **109**, 577 (1997).
 - ¹³ R.P. Feynman, *Phys. Rev.* **94**, 262 (1954).
 - ¹⁴ H.W. Jackson, and E. Feenberg, *Rev. Mod. Phys.* **34**, 686 (1962)
 - ¹⁵ H.W. Jackson, *Phys. Rev.* **A8**, 1529 (1973).
 - ¹⁶ C.C. Chang and C.E. Campbell, *Phys. Rev.* **B13**, 3779, (1976).
 - ¹⁷ B.E. Clements, E. Krotscheck, J.A. Smith and C.E. Campbell, *Phys. Rev.* **B47**, 5239, (1993).
 - ¹⁸ B.E. Clements, E. Krotscheck, C.J. Tymczak, *Phys. Rev.* **B53**, 12253, (1996).
 - ¹⁹ V. Apaja, and S. Saarela, *Phys. Rev.* **B57**, 5358 (1998) and references therein.
 - ²⁰ Deok Kyo Lee, and Felix J. Lee, *Phys. Rev.* **B11**, 4318 (1975).

- ²¹ E. Manousakis, and V.R. Pandharipande, Phys. Rev. **B33**, 150 (1986).
- ²² L.D. Landau, J. Phys. USSR **11**, 91 (1947).
- ²³ B. Fåk and J. Bossy, J. Low Temp. Phys. **112**, 1 (1998).
- ²⁴ M.R. Gibbs, K.H. Andersen, W.G. Stirling, and H. Schober, J. Phys.: Condens. Matter **11**, 603 (1999).
- ²⁵ H.R. Glyde, M.R. Gibbs, W.G Stirling, and M.A. Adams, Europhys. Lett. **43**, 422 (1998).
- ²⁶ R.J. Donnelly, J.A. Donnelly, and R.N. Hills, J. Low Temp. Phys. **44**, 471 (1981).
- ²⁷ Our experiments corroborate Ref.²⁵ in that the phonon-roton excitation energy never exceeds 2Δ upto $q = 3.6\text{\AA}^{-1}$.
- ²⁸ L.D. Landau, and I.M. Khalatnikov, Zh. Eksp. Teor. Fiz. **19**, 637 (1949).

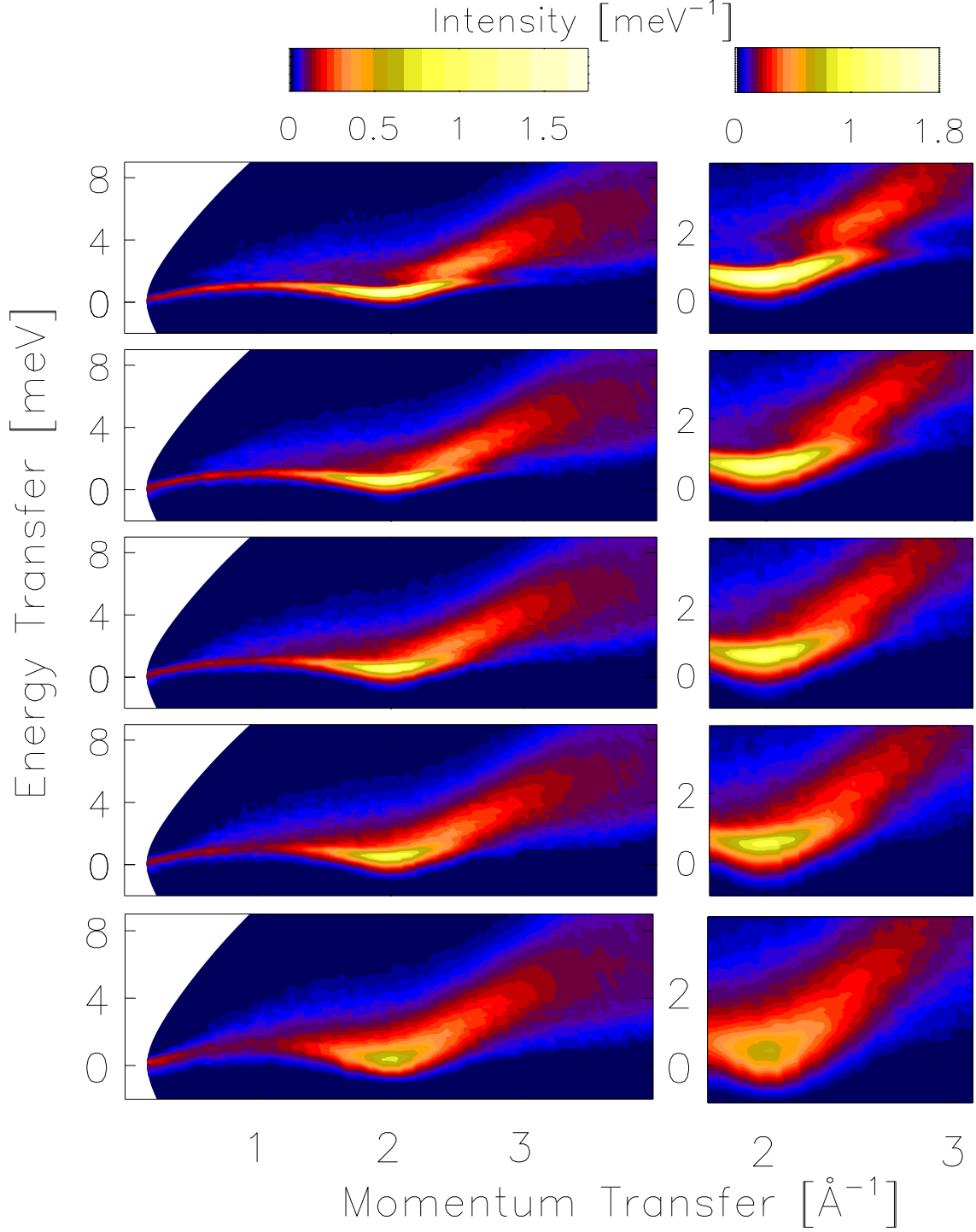


FIG. 1: The (resolution broadened) dynamic response of liquid ${}^4\text{He}$ at SVP for five temperatures ($T=1.35, 1.85, 2.0, 2.1$ and 2.3 K, from top to bottom). We also obtained results (not shown) at $2.15, T_{\lambda}-0.003$ and 3.0 K. The panels on the right show expanded views of the roton region.

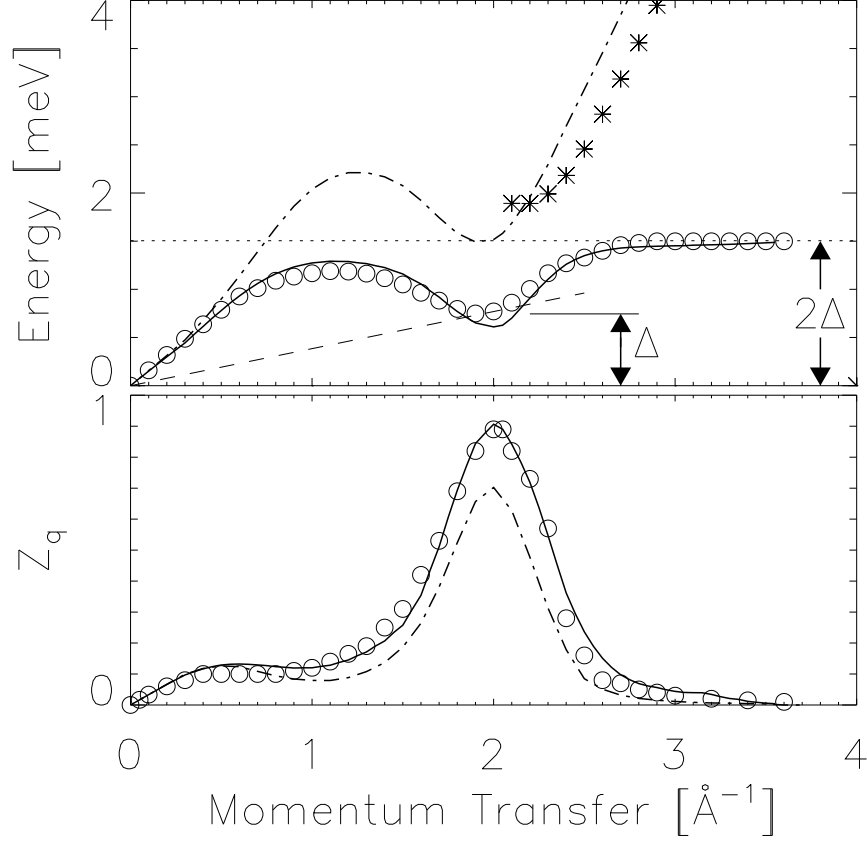


FIG. 2: Top: the phonon-roton dispersion curve of superfluid ^4He at $T < 1.3 \text{ K}$ (circles). The roton excitation is given by the minimum of the dispersion curve at $q_r = 1.92 \text{ \AA}^{-1}$, with energy gap Δ . For q -values beyond the roton, the dispersion curve asymptotically approaches 2Δ (dotted line) and terminates at about $2q_r$. The stars indicate the peak positions of the recoil component of the scattering. The uncorrected excited state energies $\hbar\epsilon_F(q)$ are given by the dashed-dotted curve, and the corrected energies (self-consistent calculation) by the solid line. Bottom: corresponding weights Z_q of the phonon-roton excitations (circles: experiment, solid line: self-consistent calculation, dashed-dotted line: simple model).

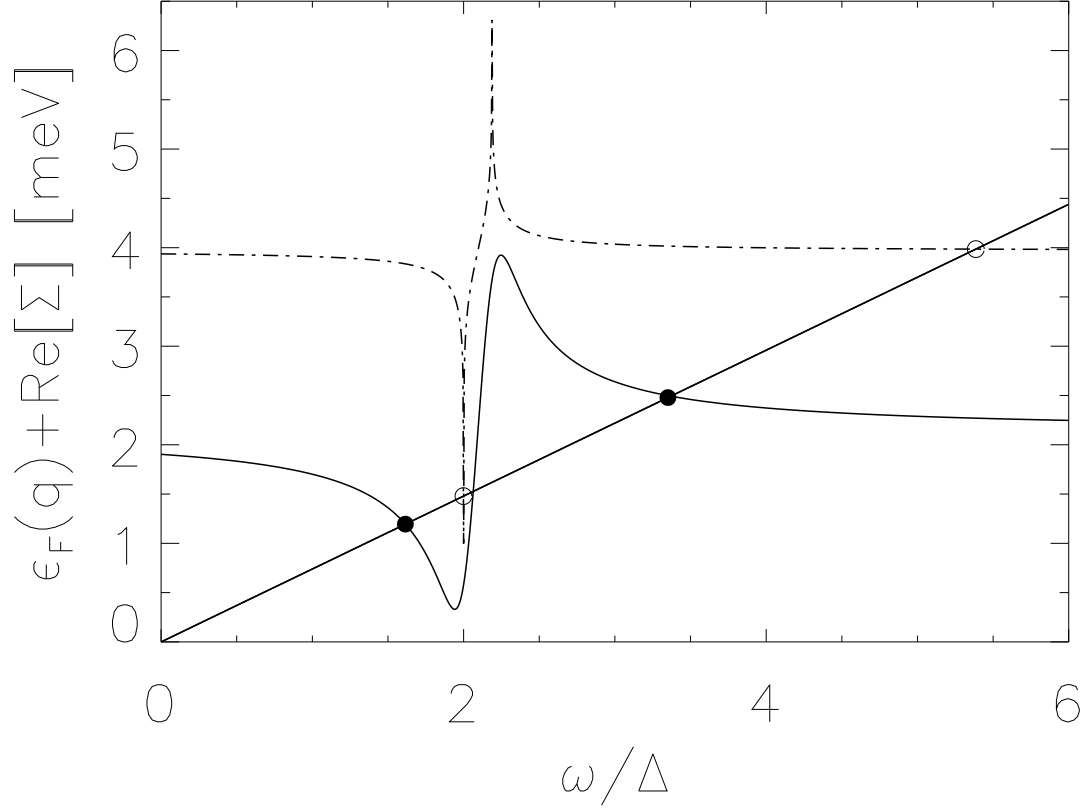


FIG. 3: Solution of the roots of $\omega + i\eta = \epsilon_F(q) + \Sigma(q, \omega + i\eta)$ for $q = 2.3$ (solid line) and 2.7 \AA^{-1} (dashed line). Only the real part of the equation is depicted here. In each case there are two solutions, shown by circles. The apparent third solution does not satisfy the imaginary part of the equation.

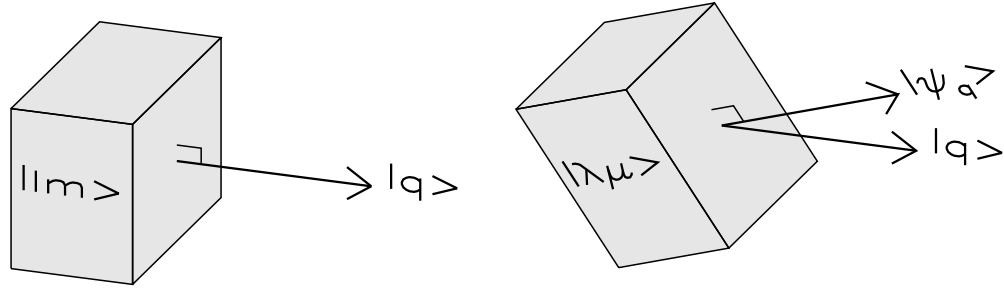


FIG. 4: Pictorial illustration of how an excited (single quasiparticle) state $|\psi_q\rangle$, which does not coincide with a simple density fluctuation $|q\rangle$, necessarily leads to the observation of multi-quasiparticle states $|\lambda\mu\rangle$.